Effect of ZrB2 and UB2 Discrete Burnable Absorber Pins on Fuel Reactivity

Bolukbasi, Mustafa; Middleburgh, Simon; Vrtiska, Scott; Lee, Bill

Progress in Nuclear Energy

DOI:
10.1016/j.pnucene.2022.104295

Published: 01/08/2022

Peer reviewed version

Effect of ZrB_2 and UB_2 Discrete Burnable Absorber Pins on Fuel Reactivity

Mustafa J. Bolukbasi[1], Simon C. Middleburgh[1], Scott Vrtiska[2], William E. Lee[1,3]

[1.] *Nuclear Futures Institute, Bangor University, Bangor, LL57 1UT, U.K.*

[2.] *Westinghouse Electric Sweden, 72163 Västerås, Sweden*

[3.] *Department of Materials, Imperial College London, London, SW7 2AB, U.K.*

Abstract

Improvements in fuel efficiency and economy are significantly important both for today's nuclear power reactors and for new, advanced nuclear reactor designs. Burnable absorbers (BA), which are a key component in fuel efficiency and economy, are being developed to improve fuel cycle flexibility and to reduce some of the performance drawbacks associated with their use. In this study, a novel concept is studied: Discrete Burnable Absorber Pins (DBAP) containing ZrB_2 and UB_2 which have immense potential for fuel efficiency and fuel cycle economy, analysed by Monte Carlo particle transport methods. It has been shown that the use of each type of discrete burnable absorber pin provides an increase in reactivity at the end of fuel life compared to the situation without a BA. This is attributed to the change in ^{239}Pu breeding in the region adjacent to the BA.

Keywords**:** Burnable absorber; Zirconium Diboride; Uranium Diboride; Monte Carlo; Advanced Technology Fuel (ATF).

1. Introduction

In nuclear design, the optimisation of efficiency and fuel economy is key to providing a reactor that has the highest possible capacity factor (OECD/NEA, 2012). By achieving higher burns and extending the nuclear fuel cycle length, planned outages days for refueling over the life of the reactor can be reduced, and thus, fuel cycle economy can be improved (Frybortova, 2019; Stewart *et al.*, 2021).

Longer fuel cycle lengths can be achieved with a combination of fuel improvements, including higher enrichment of the fuel (Durazzo et al., 2018) or loading higher uranium density fuel through the use of Advanced Technology Fuel (ATF) enhancements (Middleburgh et al., 2020). Considering that the commercial uranium enrichment limit is normally established as 5 wt.% ^{235}U (U.S.NRC, 2020), the fuel cycle length can be extended by better optimizing how the reactivity of the fuel changes with burnup, which can be achieved using neutron absorbers (Frybortova, 2019).

Burnable absorbers (hereafter called BAs) are an essential part of fuel assemblies in light water reactors (LWRs) (Ovi et al., 2021) as they absorb neutrons and prevent excessive initial reactivity at the beginning of the fuel's life (Lovecký et al., 2020). This is especially critical when replacing old fuel assemblies with new ones to rebalance the heat production in the reactor core (Papynov et al., 2020). Current commercial LWRs typically replace only a fraction of the fuel between operating cycles allowing fuel to be burned for multiple operating cycles over their life. The optimization process then involves designing BA that will result in having a desired effect on core reactivity during its first cycle of operation, but only an extremely limited effect in subsequent operating cycles. Depending on factors such as power density and operating cycle length, the ideal BA selection and design for a given set up must be adjusted

in order to achieve maximum reactivity at higher burnup. Some elements such as boron, gadolinium, dysprosium, hafnium, and erbium are used or have the potential to be used in BA materials due to their high neutron absorbing abilities (Galahom, 2016).

Gd_2O_3 is one type of BA that is used quite frequently in commercial nuclear reactors. It is used as an integral burnable absorber (IBA) in fuel pellets and in a certain number of fuel rods to cover 4-12% by weight of the fuel pellet. Of the 7 isotopes of Gd_2O_3, only 2 with a high thermal neutron capture thermal cross section are the main neutron absorbers. However, while Gd_2O_3 suppresses reactivity at the beginning of the fuel's life and provides lower initial reactivity, it also causes residual reactivity penalty due to undestroyed isotopes remaining late in the fuel's life (Khrais et al., 2019). Although there have been some studies to obtain higher reactivity at the end of the fuel's life, such as enriching it with ^{157}Gd which is the main neutron-absorbing isotope with the highest cross-section, by eliminating the residual reactivity penalty associated with Gd_2O_3, these are still preliminary (Bejmer and Seveborn, 2004; Bolukbasi et al., 2021).

Nguyen *et al.* have studied the concept of a centrally shielded burnable absorber obtained by placing the Gd_2O_3 spheres in the centre of the fuel pellets. In their study, they showed that when this concept is used as a BA solution, excessive reactivity can be controlled, and the movement of the regulating control rods can be reduced without affecting the core performance (Nguyen et al., 2019).

The thermal conductivity of the fuel pellet has a great influence on the behaviour of the fuel both under normal conditions and in unexpected situations (Evitts et al., 2020; Qin et al., 2020). During reactor operation, the temperature in the centre of the fuel pellet must be below the melting temperature of UO_2 (IAEA, 2010). Therefore, when selecting BA designs, it is also important to consider the effect on the temperature gradient from the centre of the fuel pellet, as in unexpected scenarios (such as a reactivity-initiated accident) the temperature at the centre of the UO_2 fuel pellet can quickly approach its melting point due to the low thermal conductivity of UO_2 (Suwardi, 2008). Another disadvantage of Gd_2O_3 can be its effect on further lowering thermal conductivity of the fuel.

On the other hand, the Integral Fuel Burnable Absorber (hereafter called the IFBA) concept, developed by Westinghouse Electric Company and used quite often as a BA solution (Alameri and Alrwashdeh, 2021), describes a thin ZrB_2 coating on the outer surface of the fuel pellet (Franceschini and Petrović, 2009). The thickness of this ZrB_2 layer varies according to the type of fuel used in the reactor and the enrichment amount of the fuel (Alameri and Alrwashdeh, 2021). The ^{10}B isotopes in ZrB_2 around the fuel pellet are completely depleted without causing any residual reactivity (Alameri and Alrwashdeh, 2021), resulting in a flattening of the power distribution (Amin et al., 2017). However, the rapid depletion of IFBA is not ideal for cycles more than 24 months (Choe et al., 2016; Dandi et al., 2020; Westinghouse Electric Company, 2018) and manufacturing fuel pellets with IFBA coating is quite complex and time-consuming.

Natural boron contains ^{10}B and ^{11}B isotopes (Coursey et al., 2017). During reactor operation the isotope of ^{10}B, which has a higher thermal neutron absorption cross-section (~3800 barns), captures neutrons, and as a result of the fission ^{10}B is transmuted to ^{7}Li and ^{4}He form, Eq. 1. However, residual neutron poisoning of boron is quite low compared to that of Gd isotopes (Burr et al., 2019).

$$^{10}_{5}B + ^{1}_{0}n \rightarrow ^{7}_{3}Li + ^{4}_{2}He + \gamma \qquad \text{Eq. 1}$$

On the other hand, it is possible to obtain a smoother effective multiplication constants curve with ZrB_2 compared to Gd_2O_3. Sun *et al*. stated that the rate of depletion of Gd_2O_3 is faster compared to IFBA with ZrB_2. Therefore, depending on the self-shielding and geometry of the

fuel and BA design, the Gd_2O_3 may be depleted quickly as compared to IFBA when are they introduced at equal initial reactivity during reactor operation. In addition, when the BA/total fuel ratio is kept constant and the number of rods containing BA is increased, the depletion rate of BA also increases (Sun et al., 2019).

Renier and Grossbeck stated that the use of IFBA as BA has limitations as ZrB_2 coating thickness can only be increased within certain limits. Due to this limit, it may not be possible to increase the self-shielding effect to the desired amounts, since even the maximum BA ratio that can be kept in the system may not be depleted slowly enough (Renier and Grossbeck, 2001).

UB_2 is an intermetallic material with an extremely high melting point (~2658 K). UB_2 also has a remarkably high thermal conductivity, especially when compared to UO_2 meaning that its required power to induce melting is expected to be far higher. Because of these properties, Kardoulaki *et al.* suggested that UB_2 is a relatively unexplored candidate that can replace Gd_2O_3 as BA as it does not carry some of the negative impacts that include displacing fissile material and a reduction in thermal conductivity (Kardoulaki et al., 2020; Qin et al., 2020). Burr *et al*. indicated that in addition to the thermomechanical properties of UB_2, using it as a BA prevents excessive initial reactivity by suppressing the reactivity at the beginning of the fuel's life, and thus, provides a flatter burnup because it may be integrated within the fuel pellet rather than applied to the surface of the pellet, a greater self-shielding effect may be achieved as compared to IFBA. Additionally, since it has higher uranium density than UO_2, it increases the reactivity at the end of the fuel's life (Burr et al., 2019) and increases the fuel mass which can be very desirable for commercial applications.

2. Designed model description

Enica *et al*., with the contributions of Westinghouse Electric Company, invented a new BA/pellet design to eliminate some disadvantages, negative effects, and limitations of BAs used in today's reactors (Enica et al., 2018). In their design, the BA is located as a discrete pin in the centre of the annular fuel pellet, as shown in Fig. 1. It is termed discrete as instead of being mixed homogeneously with the fuel (as with the well-used Gd_2O_3 additions to UO_2) the material containing the absorbing material (in this study ZrB_2 or UB_2) is separated from the non-absorbing material (UO_2 in this study). With UB_2, the boron absorber is kept separated from the majority of the fissile material and can again be considered discrete, despite the UB2 containing fissile uranium itself. Contrary to the IFBA, this design may allow for extended fuel cycles, beyond 24 months, by controlling the reactivity as a result of the slow depletion of the BA in the pellet center with self-shielding effect. Moreover, it increases the relatively low thermal conductivity of the UO_2 fuel pellet, which has a higher central temperature than surface during the normal reactor operation. In Fig. 1, **h** is the height and **r** is radius of fuel pellet, **r'** is the radius of the Discrete Burnable Absorber Pin (hereafter called the DBAP).

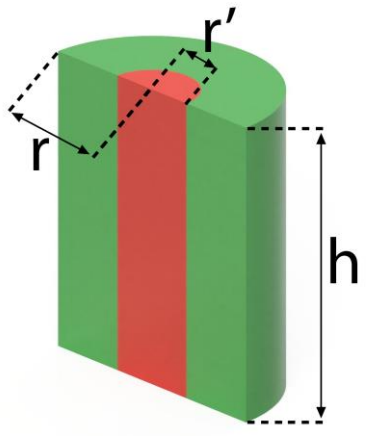

Fig. 1 Cross section of Discrete Burnable Absorber Pin (DBAP)-containing fuel pellet (green sections are UO_2 and the central red section is the BA, either ZrB_2 or UB_2 in this design. **h** is the height and **r** is radius of fuel pellet, **r'** is the radius of the DBAP.

The fuel pellet and rod designs are shown in Fig. 2 and fuel design parameters are shown in Table 1. The fuel rods containing burnable absorbers (hereafter called the BA rods) of all DBAP-containing cases are designed to have DBAPs containing ZrB_2 or UB_2 at their centre, and the radii of these DBAPs vary between 0.5 mm and 2.5 mm.

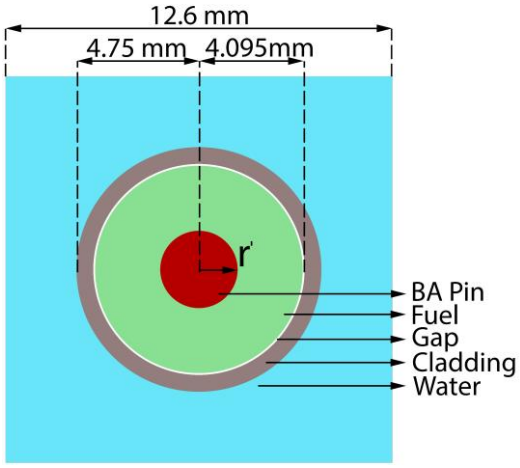

Fig. 2 Fuel pellet and DBAP designs

Table 1 Fuel design parameters.

Fuel rod pitch (mm)	12.6
Pellet radius (mm)	4.095
Rod radius (mm)	4.75
Cladding material	Zircaloy 4
Cladding thickness (mm)	0.57
UO_2 fuel density (% of TD)	95.5
BA density (both ZrB_2 and UB_2) (% of TD)	95.5

In this study, the DBAP design (Enica et al., 2018) is discussed using ZrB_2 or UB_2 as burnable absorber materials. Within this research article, neutronic analyses on this BA design was performed, the effect of the DBAP on reactivity and ^{239}Pu breeding behaviour were investigated in order to guide future studies on this design.

3. Method

Simulations were performed using The Serpent 2 Monte Carlo reactor physics code developed by VTT Technical Research Center (Leppänen et al., 2015).

Westinghouse Electric Company AP-1000 PWR reactor was chosen as a reference Nuclear Power Plant (NPP) to carry out the Serpent simulations. Other PWR systems including the European Pressurized Reactor (EPR) being built by Électricité de France (EDF) are expected to yield similar results. Some of the simulation parameters are shown in Table 2.

Table 2 Parameters used in Serpent 2 simulations

Reactor Type	PWR
Average fuel temperature (K)	900
Average cladding Temperature (K)	583
Neutron population (neutrons per cycle)	30000
Cycles (active/inactive)	300/20
IFBA coating thickness*	0.00256 cm
Rod array	17 × 17
Number of control rods	25
Number of rods with DBAP	28, 44, 72, 88 and 112

- fo

Fuel assembly designs, based on 5 different reference assemblies, are given in Fig. 3a (28 BA rods), Fig. 3b for (44 BA rods), Fig. 3c (72 BA rods), Fig. 3d (88 BA rods), Fig. 3e (112 BA rods) (Ames Ii et al., 2010). In all cases where UB_2 was used for the simulations, the ^{235}U enrichment of UB_2 was chosen equal to the ^{235}U enrichment amount in the equivalent BA-free fuel pellets.

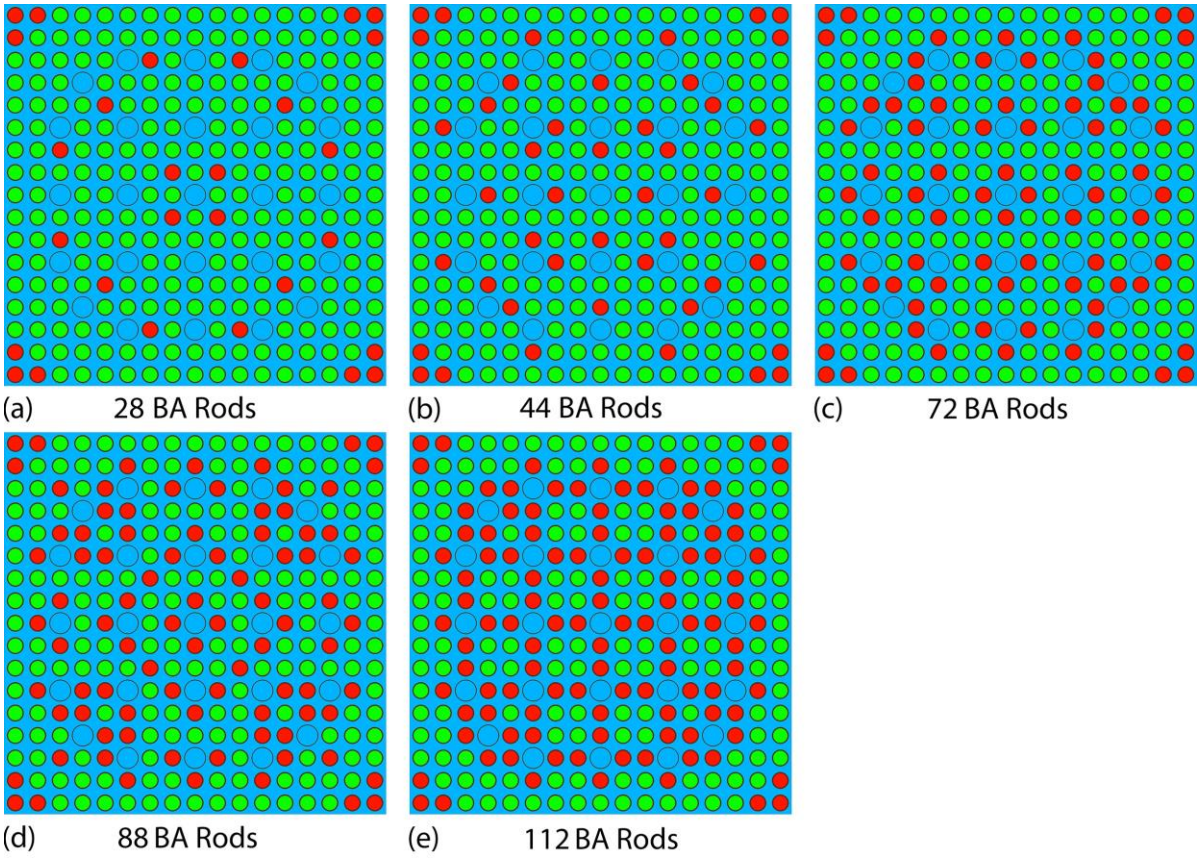

Fig. 3 Fuel assembly designs with (a) 28 BA rods, (b) 44 BA rods, (c) 72 BA rods, (d) 88 BA rods, (e) 112 BA rods used in simulations

Fuel pellets containing DBAP were examined in 5 separate equal-volume radial layers to observe the ^{239}Pu breeding behaviour in the fuel pellets as a function of radius. Likewise, the DBAPs were examined in 5 separate equal-volume radial layers to observe the changes in the isotopic composition. In addition, since the error margins of the simulations are below ±20 pcm (1 pcm = 10^{-5}), they are not indicated in the result graphs of this study.

4. Results and discussion

Fig. 4 shows the k_{inf} (infinite multiplication factor) curves of cases that have IFBA rod design (a ZrB_2 coating on the periphery of a UO_2 pellet).

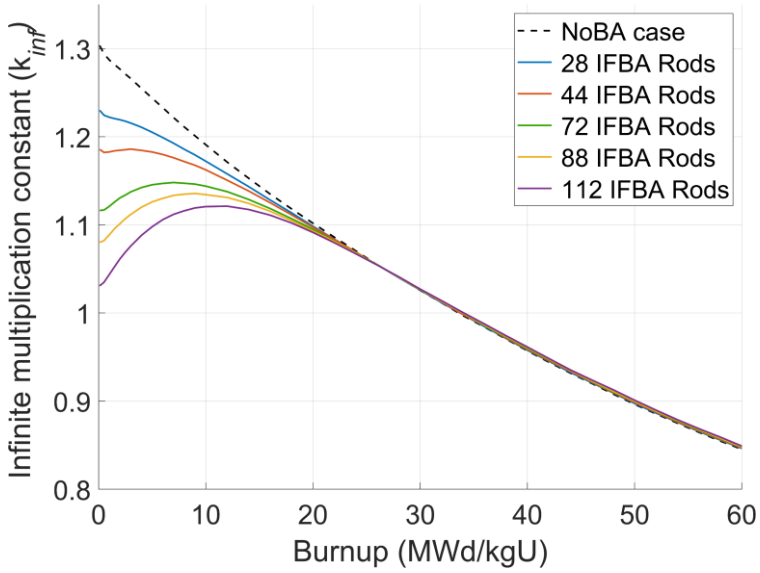

Fig. 4 Infinite multiplication constants (k_{inf}) of cases have IFBA coating in different number of rods

As can be seen in Fig. 4, the suppression on reactivity at the beginning of the fuel's life becomes more significant with the increase in the number of rods with IFBA containing pellets. In addition, after the depletion of ^{10}B isotopes in IFBA coatings, the reactivity was slightly higher than in the case without IFBA at 34 MWd/kgU (e.g., between 20 and 200 pcm depending on the number of IFBA rods).

Fig. 5a shows the k_{inf} curves of the cases with ZrB_2 (Fig. 5a) and UB_2 (Fig. 5b) DBAPs of different radii in 28 BA rods within a single assembly.

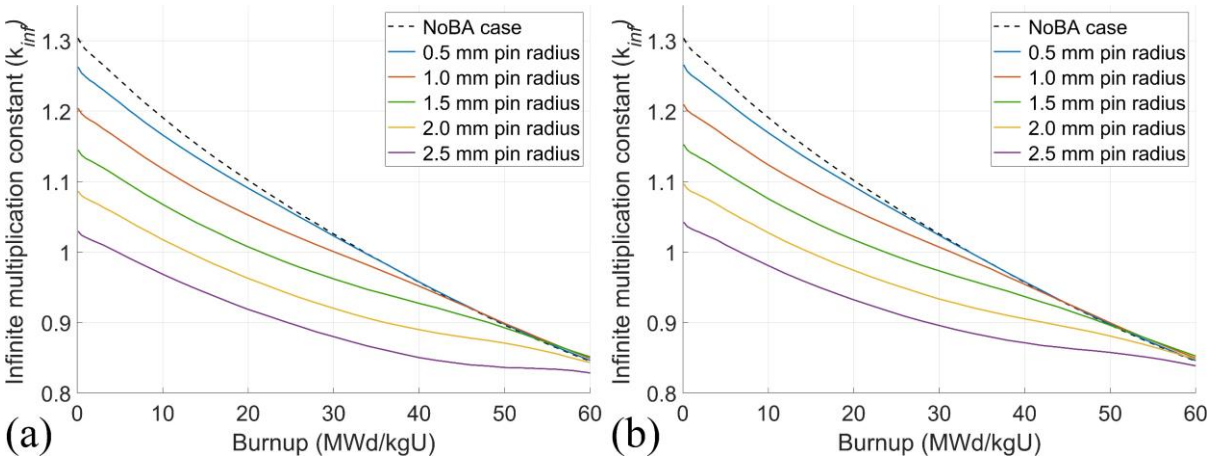

Fig. 5 Infinite multiplication constants (k_{inf}) of cases have ZrB_2 (a) and UB_2 (b) DBAPs in 28 BA rods

As can be seen in Fig. 5a and Fig. 5b, the increase in DBAP radius in the fuel pellets increases the suppression on the reactivity at the beginning of the fuel's life for both cases, ZrB_2 and UB_2 inserts. These increases also lead to higher reactivity late in the fuel's life.

On the other hand, when ZrB_2 and UB_2 DBAPs with the same radius are compared, it is seen that the reactivity is suppressed to a higher degree in cases with ZrB_2 DBAP. As the uranium in UB_2 contributes to the fission reaction as it contains fissile ^{235}U (4.45 wt. % the same

enrichment level with BA-free fuel pellets), it suppresses the reactivity less than ZrB_2 (up to 1300 PCM depending on DBAP radius).

Fig. 6 shows the k_{inf} curves of the cases with ZrB_2(Fig. 6a) and UB_2(Fig. 6b) DBAPs with a radius of 1mm of different numbers of rods in the 264 rod assembly.

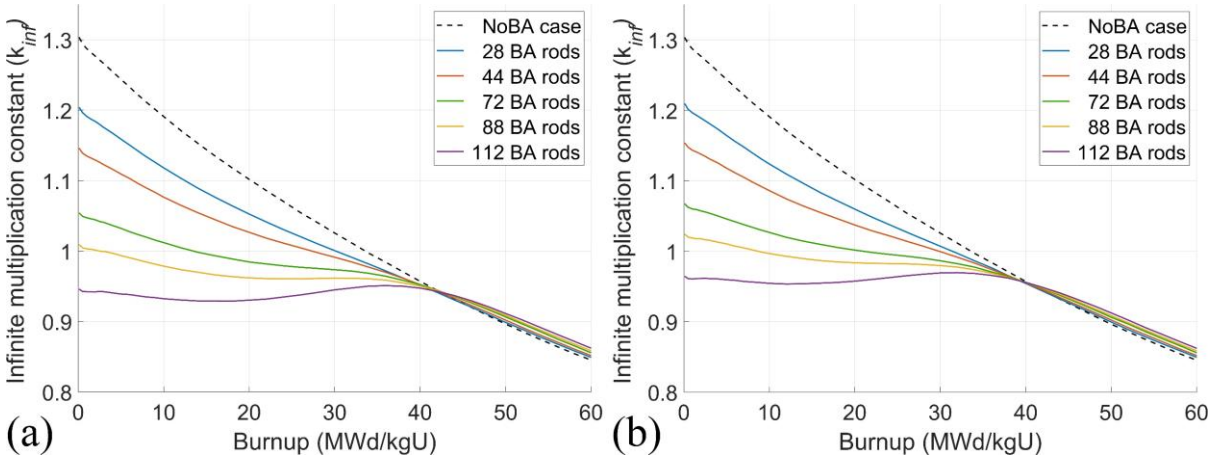

Fig. 6 Infinite multiplication constants (k_{inf}) of cases have 1mm ZrB_2(a) and UB_2(b) DBAPs in different number of BA rods

As seen in Fig. 6a and Fig. 6b, increasing the number of fuel rods with 1mm radius DBAPs increases the reduction in the reactivity at the beginning of the fuel's life, as expected, due to increase in the number of neutron absorber isotopes. In addition, after the depletion of ^{10}B isotopes within each of the borides, a higher reactivity is observed at the late stage of the fuel's life for all cases with BA, compared to the reference sample without BA which can be seen in detail in Fig A1 and Fig A2.

When the case with ZrB_2 DBAPs in 112 BA rods is observed (Fig. 6a), it is seen that the reactivity is in the subcritical state at the beginning of the fuel's life (k_{inf} = 0.9461). However, it then decreases by ~1700 PCM and reaches its lowest level before complete depletion of ^{10}B isotopes at 18 MWd/kgU. It then rises by ~2200 PCM and reaches the highest reactivity level of fuel life (at 36 MWd/kgU) and begins to decline after the depletion of most of the ^{10}B isotopes in the system. For the rest of the fuel's life, as in the other cases, it achieved higher reactivity compared to the reference case without BA. In addition, it is clearly seen that with the increasing number of BA rods, higher reactivity is obtained at the end of the fuel's life.

In the case where the UB_2 DBAPs are used in 112 BA rods (see Fig. 6b) has the same behaviour with the case with ZrB_2 DBAPs in 112 BA rods. Here again, the reactivity decreases at the early life of the fuel but then it start increasing and reaches the highest level at 36 MWd/kgU. After the depletion of most of the ^{10}B isotopes, higher reactivity is obtained for the remainder of the fuel's life compared to the case without BA. Just as in cases with ZrB_2 DBAPs, higher reactivity is achieved in the rest of the fuel's life with an increase in the number of BA rods containing UB_2 DBAPs.

Both BA compounds provided higher reactivity at the end of the fuel's life than the cases without BA. This is because, during the depletion of BA, the neutron spectrum is hardened due to the capturing of thermal neutrons. Hardening of the neutron spectrum reduces the consumption of ^{235}U, and increases the Pu breeding resulting in higher reactivity (Sanders and Wagner, 2001). Additionally, when the cases in Fig. 6a and Fig. 6b are compared, cases with ZrB_2 DBAPs shows close reactivity values with a difference of about ±20 pcm, which is in the

error margin, to each other at 50MWd/kgU. This is initially counter-intuitive until fissile isotope breeding is considered.

While the Fig. 7a shows the ^{239}Pu breeding behaviour in BA rods with ZrB_2 DBAPs (reported in Fig. 6a), Fig. 7b reveals the ^{239}Pu breeding behaviour in BA rods with UB_2 DBAPs (reported in Fig. 6b).

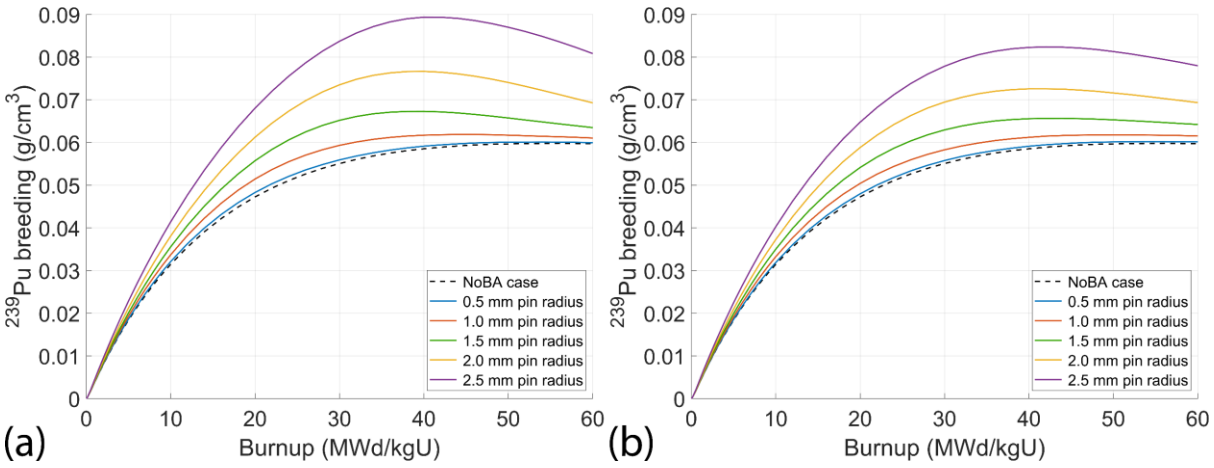

Fig. 7 ^{239}Pu breeding behaviours in BA rods with (a) ZrB_2 DBAPs, and (b) UB_2 DBAPs in 28 BA rods

As can be seen in Fig. 7, the ^{239}Pu density in the fuel composition increases depending on the increasing radius of the DBAPs due to an increasingly hardened neutron spectrum.

In cases with a ZrB_2 DBAPs with the radius of 1.0mm and above, the density of ^{239}Pu in cm^3 reaches its peak value between 32 and 40MWd/kgU. Also, the density of ^{239}Pu is almost 50% higher at 40MWd/kgU with 2.5 mm DBAP radius compared to the case that has 0.5mm DBAP radius.

When the breeding behaviour of ^{239}Pu in UB_2 DBAP-containing cases is examined, the increase in DBAP radius also increases the production of ^{239}Pu compared to the case without DBAP. However, when the cases with ZrB_2 DBAPs and UB_2 DBAPs in the same radius are compared, it is clearly seen that the density of ^{239}Pu is lower in cases containing UB_2 DBAPs.

It is obvious that the suppression on the reactivity increases due to the increasing DBAP radius and increasing number of BA rods. However, in these two increases, there is a behavioural change on k_{inf} caused by the increase of boron isotopes in the system.

For this reason, in order to see the effect of the design element on the reactivity, a series of simulations were carried out by taking two reference cases reported in Fig. 6a and Fig. 6b, which have the radius of 1.5mm DBAPs in 28 BA rods for both ZrB_2 and UB_2. By taking the BA/total-fuel ratio of these two reference cases: DBAPs in 44, 72, 88, and 112 BA rods were distributed by reducing their radius. In Fig. 8a, the k_{inf} curves of the cases where ZrB_2 DBAPs are used as BA are shown, while in Fig. 8b, the k_{inf} curves of the cases where UB_2 DBAPs are used as BAs.

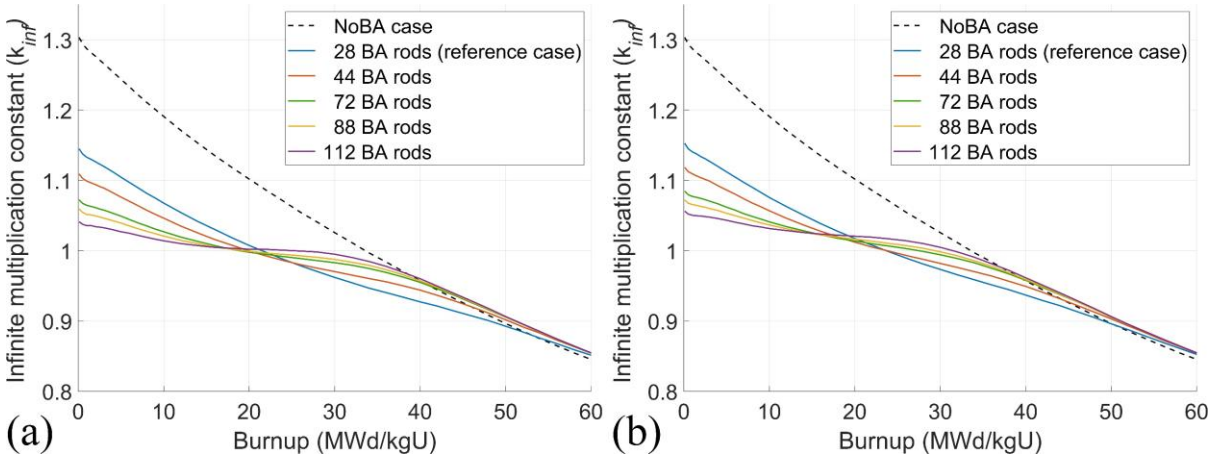

Fig. 8 Infinite multiplication constants (k_{inf}) of cases with fixed BA/total-fuel ratio; (a) ZrB_2 DBAPs, and (b) UB_2 DBAPs in different number of BA rods

As can be seen in Fig. 8a and Fig. 8b, the distribution of both ZrB_2 and UB_2 BA in a certain ratio in more rods, due to the increase in the surface area, allowing BAs to absorb neutrons at a higher rate at the beginning of the fuel's life, causing more suppression on the reactivity.

Looking at the cases with ZrB_2 DBAPs (see Fig. 8a) in detail, it is seen that reduction the radius of the DBAPs and their distribution in the assembly lead to a slower decrease of the reactivity towards the subcritical level in the fuel's life. In addition, higher reactivity occurs at the end of the fuel's life in all cases compared to the case without BA, and the reactivity is equal in all cases with BA at the end of the fuel's life.

On the other hand, when the cases using UB_2 DBAPs (see Fig. 8a) are examined in detail, it is noticed that the distribution of BA on the excess rod creates a slightly sharper distribution when compared to the reference case. This sharp difference shows itself towards the end of the assemblies' life and all cases show higher reactivity compared to the case without BA.

Graphs of the ^{239}Pu breeding behaviour of the fuel pellets on the BA rods of the cases without BA(a) and the cases with the radius of 1.5 mm ZrB_2 DBAPs (b) and UB_2 DBAPs (c) in 28 BA rods are given in Fig. 9.

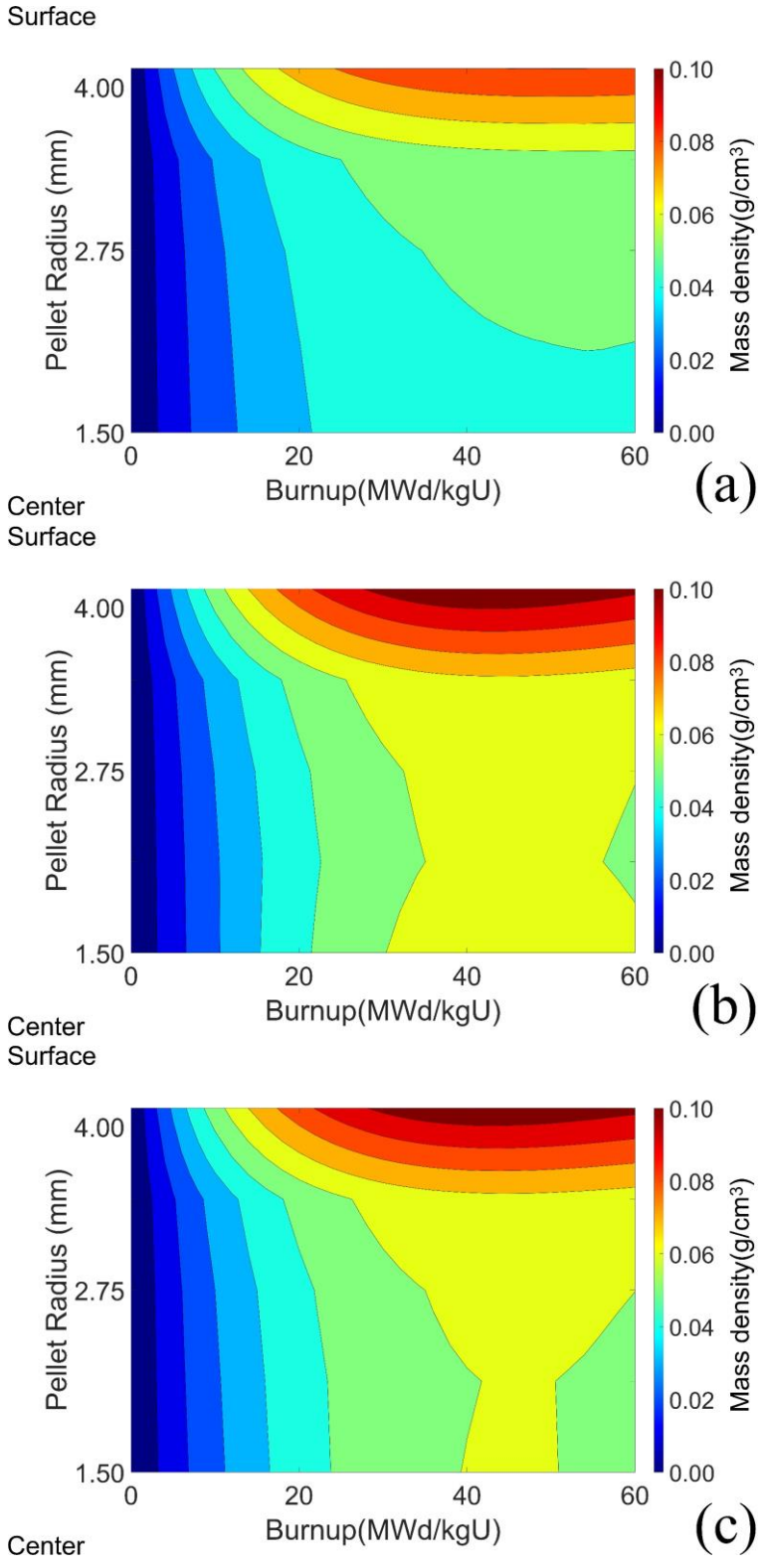

Fig. 9 ^{239}Pu breeding behaviour of cases (a) without BA, (b) with radius of 1.5 mm ZrB_2 DBAPs and (c) UB_2 DBAPs in 28 BA rods

As can be seen when Fig. 9 is examined, the mass density of ^{239}Pu in cases with DBAPs increases faster than the case without BA in all layers, and it is also faster in cases with ZrB_2 DBAPs compared to the case with UB_2 DBAPs. Just as in the case without BA, the mass density of ^{239}Pu is higher on the surface of the fuel pellets than at the centre, as determined by (Rossiter and Mignanelli, 2010). This rate becomes especially noticeable from about

26MWd/kgU and is related to the amount of ^{10}B isotopes present in the system and thus the depletion duration.

Fig. 10 shows the depletion behaviour of ^{10}B isotopes in the DBAPs of 28 BA rods with the radius of 1.5mm ZrB_2 DBAPs and the radius of 1.5mm UB_2 DBAPs.

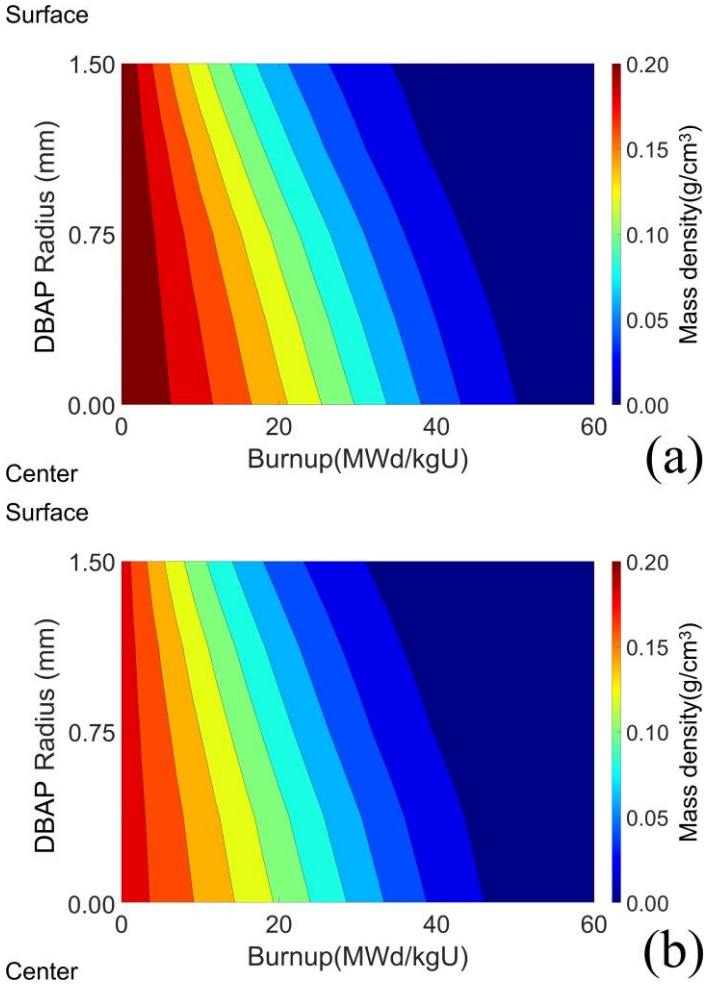

Fig. 10 Depletion behaviour of ^{10}B isotopes in the radial layers of the cases have (a) radius of 1.5mm ZrB_2 DBAPs and (b) radius of 1.5mm UB_2 DBAPs in 28 BA rods

As can be seen in Fig. 10a, the ^{10}B isotopes inside the ZrB_2 DBAPs are depleted faster on the outer surface of the DBAPs and slower in the centre. The ^{10}B isotopes are almost completely depleted at 34MWd/kgU at the outer surface of the DBAPs, while it is at ~50MWd/kgU at the centre of the pellets. This is due to the thermal neutron flux being depressed in the centre of the pellet. Note that while the ^{10}B isotopes act as a shield for uranium, the uranium will also act as a shield for the ^{10}B isotopes.

On the other hand, when Fig. 10b is examined, the ^{10}B isotopes on the UB_2 DBAPs are also depleted faster on the DBAPs surfaces than on the DBAPs centres. The ^{10}B isotopes are almost completely depleted at 31MWd/kgU at the outer surface of the DBAPs, while it is at ~46MWd/kgU at the centre of the pellets. The thermal neutron flux will be more radially homogenous within the pellet with UB_2 DBAPs as compared to ZrB_2 DBAPs.

In both DBAPs types, the ^{10}B isotopes in the system, which have high thermal neutron absorption cross-section, decay after capturing neutrons, and produce ^{4}He and ^{7}Li isotopes (see Eq. 1). For this reason, the breeding rates of ^{7}Li and ^{4}He isotopes are parallel to the depletion behaviour of ^{10}B isotopes, therefore, there is no need to consider them separately.

5. Conclusions

- As BA, the use of ZrB_2 and UB_2 DBAPs suppress the initial reactivity, as expected. Increasing the number of fuel rods with DBAPs or increasing the DBAP radius increases this suppression, due to the increasing BA ratio in the assembly.
- When they are used in the same number of BA rods with the same DBAP radius, UB_2 suppresses the reactivity at the beginning of the fuel's life less compared to ZrB_2. This is due to the presence of fissile uranium in the system, and thus, the self-shielding effect is lost earlier. Additionally, although it is expected that higher reactivity will occur in cases with UB_2 DBAPs, at the end of the fuel's life due to the presence of uranium, both ZrB_2 and UB_2 DBAP designs provides almost the same reactivity values.
- By keeping the BA/total fuel ratio constant but increasing the distribution of both ZrB_2 and UB_2 in the fuel assembly, therefore increasing the surface area of the BA in the fuel assemblies, does not cause any noticeable change at the end of the fuel's life. However, it increases the suppression on the reactivity at the beginning of the fuel's life. Therefore, the distribution of BA may be altered to flatten or peak the k_{inf} curves as desired.
- With increasing the radius of the DBAPs, the increased amount of BA in the assembly causes an increase in the density of ^{239}Pu in the system. The ZrB_2 containing DBAPs create a higher ^{239}Pu breeding level than the UB_2 DBAPs. In addition, both types of DBAPs promote faster growth of ^{239}Pu on the outer surface of the BA fuel pellets than in the centre compared to a non-BA pellet.
- The depletion rate of the ^{10}B isotopes on both DBAP designs is about 30% faster on the surface than at their centre for both BA types.
- The depletion of the ^{10}B isotopes in the fuel assembly, with both ZrB_2 DBAPs and UB_2 DBAPs, hardens the neutron spectrum, and the depletion rate of ^{235}U isotopes decreases while the breeding rate of ^{239}Pu increases both in the pellet centre and at is surface.

The use of ZrB_2 and UB_2 as DBAP has potential for use in the current generation of nuclear reactors which considers fuel enrichments below 5 wt.% uranium and cycles lengths up to 24 months long. However, in moving ^{10}B from the surface of the pellet in the case of IFBA, to the centre of the pellet in the DBAP designs, the shielding effects result in a very long-life of the BA in the system. Therefore, the DBAP concept may provide greater efficiency and economic advantages with fuels taking advantage of enrichments greater than 5wt. % ^{235}U and longer cycles than 24 months which may be targeted internationally in the near future.

Since the design on which this study was performed is relatively new and based upon modelling values, care must be taken and, when appropriate, experiments must be performed to validate the predictions and the material choices. Future studies may wish to assess the following:

- Production of ^{4}He by transmutation of ^{10}B will increase the internal pressure, the possible effects of this on the cladding integrity during operation and beyond normal conditions should be investigated.
- In addition to reactivity balance over a fuel cycle, safety, shutdown and thermal margins should also be examined, as well as radial and axial neutron flux and power distributions, by performing 3D full core analyses.
- The manufacturing costs of fuel pellets with ZrB_2 and UB_2 DBAPs should be determined and compared to IFBA concepts. This will aid analysis into the benefits of the designs related to the levelized cost of electricity of a particular reactor and can be investigated by using methods including full 3D core analysis.
- The usage scenarios of DBAPs with lower radius should be investigated by examining the results that can be obtained by enriching the ^{10}B concentration in the DBAP for both

DBAPs since the amount of uranium that can be loaded will increase with the decreasing DBAP radius, and thus, it is possible to reach a higher rate of burnup.

- Material interaction between the DBAP and the UO_2 pellet throughout the lifetime of the pellet needs assessing, and a suitable barrier engineered if necessary.
- The behaviour of the DBAP during accident or anticipated operational occurrences needs assessing, taking into account properties such as the melting point, thermal expansion, and alterations to the specific heat capacity of the fuel.

Acknowledgements

The authors would like to express their gratitude to the Turkish Republic's Ministry of National Education. We also acknowledge the VTT Technical Research Centre of Finland and the OECD NEA Data Bank for making Serpent 2 available. All calculations in this study were performed on Supercomputing Wales. SCM and WEL are funded through the Sêr Cymru II programme by Welsh European Funding Office (WEFO) under the European Development Fund (ERDF).

References

Alameri, S.A., Alrwashdeh, M., 2021. Preliminary three-dimensional neutronic analysis of IFBA coated TRISO fuel particles in prismatic-core advanced high temperature reactor. Ann. Nucl. Energy 163, 108551. https://doi.org/10.1016/j.anucene.2021.108551

Ames Ii, D.E., Tsvetkov, P. V, Rochau, G.E., Rodriguez, S., 2010. High Fidelity Nuclear Energy System Optimization Towards an Environmentally Benign, Sustainable, and Secure Energy Source. https://doi.org/10.2172/992769

Amin, E.A., Bashter, I.I., Hassan, N.M., Mustafa, S.S., 2017. Fuel burnup analysis for IRIS reactor using MCNPX and WIMS-D5 codes. Radiat. Phys. Chem. 131, 73–78. https://doi.org/10.1016/j.radphyschem.2016.10.019

Bejmer, K.H., Seveborn, O., 2004. Enriched Gadolinium as Burnable Absorber for PWR. Proc. PHYSOR Phys. Fuel Cycles Adv. Nucl. Syst. - Glob. Dev.

Bolukbasi, M.J., Middleburgh, S.C., Dahlfors, M., Lee, W.E., 2021. Performance and economic assessment of enriched gadolinia burnable absorbers. Prog. Nucl. Energy 137, 103752. https://doi.org/10.1016/j.pnucene.2021.103752

Burr, P.A., Kardoulaki, E., Holmes, R., Middleburgh, S.C., 2019. Defect evolution in burnable absorber candidate material: Uranium diboride, UB2. J. Nucl. Mater. 513, 45–55. https://doi.org/10.1016/j.jnucmat.2018.10.039

Choe, J., Shin, H.C., Lee, D., 2016. New burnable absorber for long-cycle low boron operation of PWRs. Ann. Nucl. Energy 88, 272–279. https://doi.org/10.1016/j.anucene.2015.11.011

Coursey, J.S., Schwab, D.J., Tsai, J.J., Dragoset, R.A., 2017. Atomic Weights and Isotopic Compositions for All Elements, NIST Physical Measurement Laboratory.

Dandi, A., Lee, M.J., Kim, M.H., 2020. Feasibility of combinational burnable poison pins for 24-month cycle PWR reload core. Nucl. Eng. Technol. 52, 238–247. https://doi.org/10.1016/J.NET.2019.07.026

Durazzo, M., Freitas, A.C., Sansone, A.E.S., Ferreira, N.A.M., de Carvalho, E.F.U., Riella, H.G., Leal Neto, R.M., 2018. Sintering behavior of UO2–Er2O3 mixed fuel. J. Nucl. Mater. 510, 603–612. https://doi.org/10.1016/j.jnucmat.2018.08.051

Enica, A., Middleburgh, S.C., Vrtiska, S.J., 2018. Annular Nuclear Fuel Pellets with Discrete Burnable Absorber Pins. US2018330832A1.

Evitts, L.J., Middleburgh, S.C., Kardoulaki, E., Ipatova, I., Rushton, M.J.D., Lee, W.E., 2020. Influence of boron isotope ratio on the thermal conductivity of uranium diboride (UB2) and zirconium diboride (ZrB2). J. Nucl. Mater. 528, 151892. https://doi.org/10.1016/j.jnucmat.2019.151892

Franceschini, F., Petrović, B., 2009. Fuel with advanced burnable absorbers design for the IRIS reactor core: Combined Erbia and IFBA. Ann. Nucl. Energy 36, 1201–1207. https://doi.org/10.1016/j.anucene.2009.04.005

Frybortova, L., 2019. VVER-1000 fuel cycles analysis with different burnable absorbers. Nucl. Eng. Des. 351, 167–174. https://doi.org/10.1016/j.nucengdes.2019.05.026

Galahom, A.A., 2016. Investigation of different burnable absorbers effects on the neutronic characteristics of PWR assembly. Ann. Nucl. Energy 94, 22–31. https://doi.org/10.1016/j.anucene.2016.02.025

IAEA, 2010. Advanced fuel pellet materials and fuel rod design for water cooled reactors. Tech. Comm. Meet. held Villigen 241.

Kardoulaki, E., White, J.T., Byler, D.D., Frazer, D.M., Shivprasad, A.P., Saleh, T.A., Gong, B., Yao, T., Lian, J., McClellan, K.J., 2020. Thermophysical and mechanical property assessment of UB2 and UB4 sintered via spark plasma sintering. J. Alloys Compd. 818, 153216. https://doi.org/10.1016/j.jallcom.2019.153216

Khrais, R.A., Tikhomirov, G. V., Saldikov, I.S., Smirnov, A.D., 2019. Neutronic analysis of VVER-1000 fuel assembly with different types of burnable absorbers using Monte-Carlo code Serpent. J. Phys. Conf. Ser. 1189. https://doi.org/10.1088/1742-6596/1189/1/012002

Leppänen, J., Pusa, M., Viitanen, T., Valtavirta, V., Kaltiaisenaho, T., 2015. The Serpent Monte Carlo code: Status, development and applications in 2013. Ann. Nucl. Energy 82, 142–150. https://doi.org/10.1016/j.anucene.2014.08.024

Lovecký, M., Závorka, J., Jiřičková, J., Škoda, R., 2020. Increasing efficiency of nuclear fuel using burnable absorbers. Prog. Nucl. Energy 118. https://doi.org/10.1016/j.pnucene.2019.103077

Middleburgh, S., Bolukbasi, M., Goddard, D., 2020. Enhancing economics with ATF. Nucl. Eng. Int. Mag. 24–27.

Nguyen, X.H., Kim, C.H., Kim, Y., 2019. An advanced core design for a soluble-boron-free small modular reactor ATOM with centrally-shielded burnable absorber. Nucl. Eng. Technol. 51, 369–376. https://doi.org/10.1016/j.net.2018.10.016

OECD/NEA, 2012. The Economics of Long-term Operation of Nuclear Power Plants.

Ovi, M.H., Shelley, A., Prodhan, M.H., 2021. Neutronic analysis of VVER-1000 MOX fuel assembly with burnable absorber Gadolinia and Erbia. Ann. Nucl. Energy 160, 108389. https://doi.org/10.1016/j.anucene.2021.108389

Papynov, E.K., Shichalin, O.O., Buravlev, I.Y., Portnyagin, A.S., Mayorov, V.Y., Belov, A.A., Sukhorada, A.E., Gridasova, E.A., Tananaev, I.G., Sergienko, V.I., 2020. UO2-Eu2O3 compound fuel fabrication via spark plasma sintering. J. Alloys Compd. 155904. https://doi.org/10.1016/j.jallcom.2020.155904

Qin, M.J., Middleburgh, S.C., Cooper, M.W.D., Rushton, M.J.D., Puide, M., Kuo, E.Y., Grimes, R.W., Lumpkin, G.R., 2020. Thermal conductivity variation in uranium dioxide

with gadolinia additions. J. Nucl. Mater. 540, 152258. https://doi.org/10.1016/j.jnucmat.2020.152258

Renier, J.-P.A., Grossbeck, M.L., 2001. Development of Improved Burnable Poisons for Commerical Nuclear Power Reactors.

Rossiter, G., Mignanelli, M., 2010. The characteristics of LWR fuel at high burnup and their relevance to AGR spent fuel. Natl. Nucl. Lab. (10) 10930, 1–60.

Sanders, C.E., Wagner, J.C., 2001. Impact of Integral Burnable Absorbers on PWR Burnup Credit Criticality Safety Analyses. NCSD Conference Paper.

Stewart, R., Blakely, C., Zhang, H., 2021. Investigation of a two-year cycle pressurized water reactor core design with increased enrichment and extended burnup limits. Nucl. Eng. Des. 376, 111132. https://doi.org/10.1016/j.nucengdes.2021.111132

Sun, Y., Yang, Q., Gao, J., Liu, C., Jin, M., 2019. Research on the application of burnable poison ZrB2 and Gd2O3 in a small modular lead-based thermal reactor. Ann. Nucl. Energy 124, 21–27. https://doi.org/10.1016/j.anucene.2018.09.012

Suwardi, 2008. Thermal Performance Prediction of UO2 Pellet Partly Containing 9 % w Tungsten Network, in: International Conference on WWER Fuel Performance.

U.S.NRC, 2020. Increased Enrichment [WWW Document]. URL https://www.nrc.gov/reactors/atf/enrichment.html

Westinghouse Electric Company, 2018. Nuclear Fuel - Integral Fuel Burnable Absorber (IFBA) Fuel Cycles and IFBA/Gad Hybrid Fuel Cycles.

Appendix A.

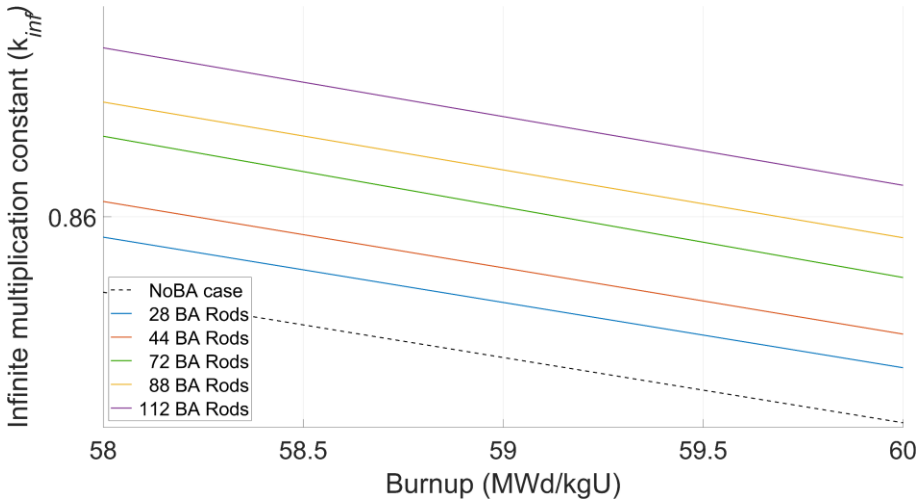

Fig A1 k_{inf} curves between 58 and 60 MWd/kgU of cases have ZrB_2 DBAPs

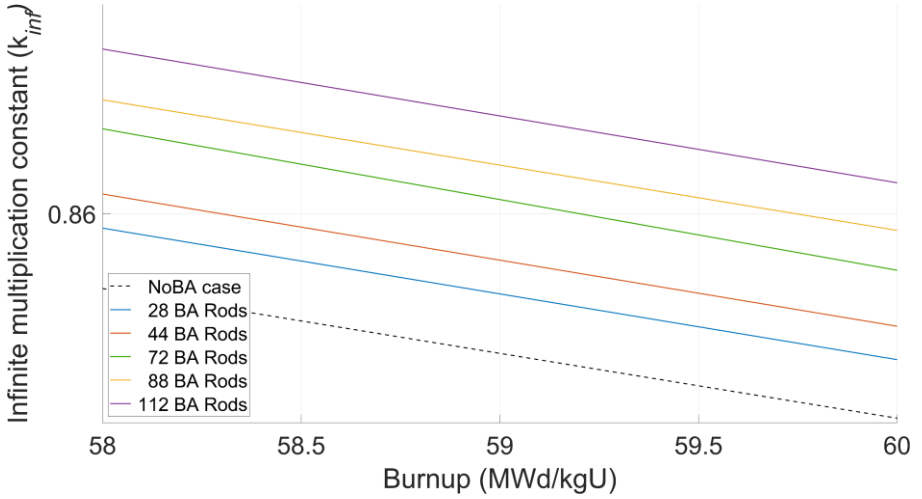

Fig A2 k_{inf} curves between 58 and 60 MWd/kgU of cases have UB_2 DBAPs